heritage

MDPI

Article

Looking at the Modern to Better Understand the Ancient: Is It Possible to Differentiate Mars Pigments from Archaeological Ochres?

Maria Cecilia Carangi [1,*], Cristina Corti [2,3] and Laura Rampazzi [2,3,4]

[1] Department of Architecture and Urban Studies, Politecnico di Milano, Via Bonardi 3, 20133 Milano, Italy
[2] Department of Human Science and Innovation for the Territory, University of Insubria, Via Sant'Abbondio 12, 22100 Como, Italy; cristina.corti@uninsubria.it (C.C.); laura.rampazzi@uninsubria.it (L.R.)
[3] Centre for Cultural Heritage Studies, University of Insubria, Via Sant'Abbondio 12, 22100 Como, Italy
[4] Institute of Heritage Science, National Research Council (ISPC-CNR), Via Cozzi 53, 20125 Milano, Italy
* Correspondence: mariacecilia.carangi@polimi.it

Abstract: This article offers a discussion of the possibility of distinguishing ochres from Mars pigments. The discussion addresses technological, archaeological, and artistic aspects. Natural earth pigments such as ochres, siennas, and umbers have been widely used from the Paleolithic to the present day and still find wide application despite the development of synthetic iron oxide pigment synthesis processes, called Mars pigments. The potential ability of today's analytical techniques to distinguish between two classes of pigments of the same color with very similar chemical composition—but perhaps sufficient for reliable recognition—is also discussed. The paper begins by addressing the proper use of the terms "ochres" and "Mars pigments" and their accurate identification in artworks. It reviews the literature on the chemical–mineralogical characterization of yellow and red iron pigments and analyzes pigment catalogs to understand how companies distinguish ochres from Mars pigments. An experimental analysis using External Reflection Infrared Spectroscopy (FTIR-ER) compared painting samples made with natural ochres and Mars pigments, confirming the literature findings and suggesting future research directions. Key differences such as hematite in yellow ochres and specific spectral peaks in red ochres support the potential of FTIR-ER spectroscopy as a noninvasive tool for distinguishing pigments, especially for fragile artifacts and archaeological applications.

Keywords: ochres; Mars pigments; archaeometry; infrared spectroscopy; yellow pigments; red pigments

Citation: Carangi, M.C.; Corti, C.; Rampazzi, L. Looking at the Modern to Better Understand the Ancient: Is It Possible to Differentiate Mars Pigments from Archaeological Ochres? *Heritage* **2024**, *7*, 6192–6212. https://doi.org10.3390//heritage7110291

Academic Editor: Silvano Mignardi

Received: 2 October 2024
Revised: 29 October 2024
Accepted: 1 November 2024
Published: 4 November 2024

1. Introduction

Color has always been one of the primary means used by humans to communicate events or states of mind. From the earliest forms of figurative expression, dating back to the Paleolithic with cave paintings, the search for coloring substances or means has been a typical activity of every civilization, from primitive ones onward. Initially, natural mineral and vegetable sources (such as charcoal, earth, or rocks) were used, and with scientific progress, suitable means for chromatic expression were synthesized [1–4]. Ochres are stable pigments: resistant to light, oxidation, and corrosion, with low reactivity with other pigments and external pollutants. They are characterized by good covering power, low toxicity, and the ability to cover a wide chromatic spectrum (yellow, orange, red, brown, and violet) depending on their mineral composition, impurities, and formation conditions. Thanks to these characteristics, ochres are still widely used today; they can be found in the palettes of contemporary artists and are also used in the construction, coatings, and paint industries despite the development of the synthetic pigment industry [5].

Ochre pigments are a natural mixture of iron oxides and clays, combined with other accessory components such as calcite, gypsum, quartz, or other mineral oxides. The

presence of manganese oxide separates ochres from siennas and umbers [1,3,6]. Pigments which may be classed as ochres can be found globally. Their exact composition and, consequently, their color and working properties are highly specific to their local geological conditions. Significant producers of ochre pigments include France, Spain, Cyprus, Iran, Italy, Australia, and the USA [6].

Iron oxides can be present in varying amounts, mainly as goethite (α-FeOOH), hematite (α-Fe_2O_3), magnetite (Fe_3O_4), maghemite (γ-Fe_2O_3), and lepidocrocite (γ-FeOOH) [7]. In yellow ochres, the main chromophore is goethite, while in red ochres, hematite is more prevalent. The color of these materials has been attributed to the light absorption due to ligand–metal charge transfer between the Fe^{3+} ion and its O^{2-} or OH^- ligands, influenced by field d–d transitions [5,7,8]. Since prehistoric times, ochres have been used either alone, by pulverizing the extracted mineral, or by mixing them with other minerals to achieve a precise chromatic gradation. Additionally, they could undergo thermal treatments to further modify the color, yielding artificial red ochres [8,9]. Evidence of thermal treatment of coloring materials is not well documented, and it is still unclear whether the earliest forms of cooking yellow ochres to obtain red or brown pigments were intentional or not. At temperatures between 350 and 400 °C, the reaction that dehydrates goethite and transforms it into disordered hematite occurs. To achieve the crystalline form of the chromophore, temperatures close to 800/900 °C are necessary. Mastrotheodoros and Beltsios, 2022 [8], highlighted that this process was carried out due to the scarce presence of pure hematite and the difficulty encountered in grinding the hematite mineral. Later, throughout the centuries, the search for new methods of producing ochres from other iron-rich minerals began, primarily for alchemical purposes. To produce yellow ochres, methods were studied that allowed the incorporation of the hydroxyl group into iron oxides. The production of artificial red ochres remained mainly tied to the firing of yellow ochres for centuries despite the existence of alternative methods based either on the firing of ferrous sulfates or other iron salts or on the dissolution of ferrous compounds followed by drying and calcination. To produce brown and violet ochres, manganese dioxide (MnO_2) or carbon black was added to further darken the color. Despite these descriptions, the processes for producing artificial iron pigments, known as Mars pigments, became widely disseminated towards the end of the 18th century.

From that time to now, the use of Mars pigments has been documented in painters' palettes. Fragoso et al. (2016) [10] found the use of Mars pigments (yellow, red, and black) in the painting *The Hermit* by Antonio Dacosta (1914–1990). Townsend (1993) [11] characterized the pigments of J.M.W. Turner (1775–1851) found in his studio after his death and highlighted the presence of Mars pigments. Kampasakali et al. (2007) [12] studied the pigments used by some Russian avant-garde painters. Their analyses revealed the presence of yellow, red, and black iron-based pigments, but they could not determine whether they were ochres or Mars pigments. In many other articles consulted, the terms *ochre* and *Mars pigments* were often used as synonyms, making it more challenging to understand the type of material chosen by the artist. The choice of one term over the other is not explained at all. Moreover, it is surprising how few articles report the recognition of Mars pigments even in artworks created during a period when they were presumably present in many painters' palettes. The literature, therefore, indicates the urgency of clarifying the issue. The differentiation between ochres and Mars pigments goes beyond the correct use of terminology, as it implicitly indicates the technology of pigment preparation and provides valuable information about the period of execution of the artwork. Additionally, it could provide information about the authenticity of an archaeological artwork or the presence of undocumented restoration or conservation interventions, which are useful for reconstructing the conservation history of the work of art and the history of past restoration techniques [13–15].

The paper looks at the modern to better understand the ancient: Starting from an in-depth literature review focused on the use of the term *Mars pigment* and the chemical-mineralogical characterization techniques used, we sought to learn the criteria adopted by

researchers to distinguish Mars pigments from ochres. Beyond the purely technological, historical, and artistic aspects, the potential capability of analytical techniques to distinguish between two classes of pigments of the same color with a very similar chemical composition—but perhaps sufficient for reliable recognition—is discussed herein. The aim is the research of analytical ways to recognize restorative interventions or forgeries in archaeological artifacts where modern synthetic pigments have been used to integrate or imitate natural ones, respectively. The study begins with a survey of the correct use of the terms *ochres* and *Mars pigments* and their accurate identification in artworks, from archaeological objects to modern paintings, a period that coincides with the spread of Mars pigments. Our research conducted in the catalogs of the main companies selling pigments is laid out to elucidate the specifications used by companies to label a product as *ochre* rather than *Mars pigment*. Finally, the results obtained from a comparison between Mars pigments and ochres, both as such and applied on a substrate, are discussed. The analysis, conducted by infrared spectroscopy, is intended to experimentally verify the results of the literature search and to propose possible avenues of investigation.

1.1. Natural Ochres: Analytical Characterization

Articles discussing the chemical characterizations of archaeological ochres and ochres used in more recent times were reviewed.

Aura Tortosa et al., 2021 [16], analyzed some ochres dating from the Paleolithic-Mesolithic period in Spain. The research highlighted that the composition of archaeological ochres was so varied that major chromophores are often present even in much lower concentrations than other minerals. The same was observed in the study carried out on archaeological findings from the Hoabinhian complex (Vietnam) [17] and on Neolithic ochres from Clearwell Caves and Çatalhöyük [18]. The presence of maghemite was detected in decorated Neolithic ceramics in addition to the accessory minerals [19]. The authors concluded that its presence could be associated with the production of red ochre by firing yellow ochres rather than using natural red. The literature reports that the most common accessory minerals in ochres are kaolinite [7,17,20–22], quartz [7,17–23], and calcite [7,16,17,19,20,23–25] and more generally silicates [18,21,23,25], clays [20,22,24], and sulfates [21]. The most frequently used techniques for the identification of ochres were Raman and FTIR spectroscopy [17,19–24], XRD [17–19,21–23], and XRF [17,23]. Infrared spectroscopy was used to a much lesser extent.

1.2. Mars Pigments: Historical Sources

At the end of the 18th century, new and efficient methods for producing iron pigments with high covering power and uniform particle size, which were also much purer than ochres, were introduced [11,26]. Harley, 1892 [27], highlighted that Mars pigments derive their name from the Latin *crocus martis*, used by alchemists since ancient times to refer to yellow iron oxide. The term *crocus* was associated with the saffron yellow color, and *martis* was internationally used to refer to iron (due to Mars, the God of War) [28]. Although alchemists began working on synthetic yellow iron pigments several centuries earlier, there are not many references to artists using these pigments. Harley (1892) [27] believed this might be due to the high availability of yellow ochre, making a synthetic version unnecessary. Consequently, their subsequent spread might be more due to the development of the chemical industry rather than an actual need for synthetic materials like ochres. The first reference to Mars yellow was found in a patent from 1780, where it was called *oker*, and later, in a 1794 specification, it was referred to as *crocus martis* or *saffron of Mars*.

The first recipe for Mars pigments synthesis, written by Jacques Blockx, dates to 1865 [6,27]. Generally, they are obtained by precipitating a solution containing a soluble iron salt and alum (to obtain a light yellow) with an alkali, such as soda or lime; the product is then dried at low temperature to avoid altering its color. Extenders such as carbonates, gypsum, or barite or other organic and inorganic pigments are often added to the pigment to enhance its intensity. Currently, the preferred synthesis method requires

the precipitation and hydrolysis of iron salts with subsequent oxidation with an aromatic nitrogen compound in the presence of hydrolyzable multivalent salts [6,29–31].

Mars yellow, FeOOH, the first pigment in this category to be synthesized, can exist in a variety of distinct crystalline forms, with the most used in painting being goethite and lepidocrocite. Goethite, α-FeOOH, is the most common form that iron oxide can take and belongs to the jasper group; it is a dark brown or black mineral from which a yellow powder of various shades can be obtained depending on particle size, and it takes its name from the German writer Goethe [6]. In 1996, Cornell and Schwertmann [1] described several synthesis routes, the most common of which involve iron sulfide or ferric nitrate as the starting reagent [6]. Lepidocrocite, γ-FeOOH, from the Greek λεπίς κροκη, meaning *saffron-colored flakes*, is instead yellow-orange, with an orthorhombic layered crystalline structure held together by hydrogen bonds. It is commonly found in rust and soils but is much less abundant than goethite and hematite. Several synthesis routes have also been found for this mineral, one of which involves the precipitation of ferrous hydroxide followed by oxidation.

Red Mars can be obtained by calcination of Mars yellow. Mars red is an iron oxide with the formula Fe_2O_3. This brick red pigment's shade depends on granularity, calcination, and the possible presence of other pigments with which it is mixed. It ensures stability in light and has significant chemical inertia [3]. Here too, different crystals with the same empirical formula can be distinguished. Hematite (α-Fe_2O_3), the most common, is a mineral that produces a bright-red powder with a rhombohedral crystalline structure. It can be synthesized in multiple ways, although calcination or dehydration of Mars yellow is generally preferred, a process that converts iron oxide-hydroxide into iron (III) oxide. Heating goethite to a high temperature, around 350–400 °C, leads to the formation of a disordered form of hematite that then evolves into ferric oxide once about 900 °C is reached, with the migration of cations present in the mineral to their sites in the structure. Other synthesis methods described in 1996 by Cornell and Schwertmann include reacting a hydrochloric acid solution with ferric nitrate enneahydrate at 98 °C or heating iron sulfate hydrate alone or with calcium oxide [6]. Calcining lepidocrocite, on the other hand, initially yields maghemite (γ-Fe_2O_3), a dark red iron oxide, which, with further temperature increase, recrystallizes as hematite. Maghemite can be also obtained by firing Mars yellow (or yellow ochres) in a reducing atmosphere.

2. Literature Review

Eastaugh et al. proposed useful definitions of the two classes of pigments [6]:

Ochres are defined as a "*variably coloured rocks and soils primarily composed of oxides and hydroxides of iron. Colours can vary through various shades of purple, red, orange and yellow. Ochres are secondary deposits occurring either as soils or 'gossans' (the weathered, highly oxidised surface outcrops of ore deposits) which have become enriched in the colour-bearing constituent, usually iron oxides or iron hydroxides. The presence of such minerals promotes a strong and permanent colour, which due to the micron-scale grain size of the particles is not reduced on grinding*".

On the contrary, Mars pigments are "*a group of synthetically produced iron oxide pigments with colours in the yellow-red-violet-black range, the term typically qualified by a colour descriptor (such as 'Mars red'). The mars colours emerged in the eighteenth century*".

Based on these definitions, characterization studies of pigments used to produce artistic artifacts were searched for in the literature. Articles in which the presence of Mars pigments was identified were selected, and the methodology followed by the authors to differentiate such pigment from ochres was critically reviewed. In addition, it was evaluated whether the use of the term Mars pigment was truthful or the result of possible misunderstanding of the term. The selected articles are shown in Table 1.

Table 1. Bibliography reporting on the recognition of Mars pigments in works of art. For each reference, the work of art analyzed and the date it was made, the ochres and/or Mars pigments recognized, the analytical techniques used, and the rationale on the use of the two terms are given.

Reference	Where the Pigments Come from?	Which Techniques Were Used?	Which Pigments Were Identified?	Are Ochres also Present?	Why Identified as Mars Pigment?
Čukovska et al., 2012 [32]	48 samples from Dicho Zograph's (1819–1872) wall paintings.	Optical microscopy, μ-Raman, GC/MS.	Mars red, Mars yellow.	Red ochre, yellow ochre.	The pigments used by the artist are not identified as natural (ochre) or synthetic (Mars) because it is possible that both are used. Red ochre can be differentiated from Mars red by a Raman peak around 660 cm^{-1}, present in some red ochres.
Fragoso et al., 2016 [10]	*The Heremit of António Dacosta*, from 1985. Acrylic on canvas.	Digital X-ray radiograpy, XRF, Dark-field microscopy, SEM-EDX, μ-Raman.	Mars yellow, Mars red.	Not found.	Not explained.
Franquelo et al., 2009 [24]	*Lady Santa Ana*, polychromed sculpture, XIV century; *Saint Pascual Bailon*, *Saint Francis of Assisi*, and *the Virgin Maria*, sculptures by Martinez Montañes, XVII century; *Virgin and the Child*, by Murillo, XVII century; *A portrait collection of carmelitas Saints*, XVII century; Paintings by Mohedano, XVIII century; Wall paintings from the House of the Golden Bracelet, Pompeii, II century BCE; Wall paintings from Cartuja Monastery, XVI and XVII centuries; El Salvador Church, XIX century.	Cross-sections with stereomicroscope, FTIR absorbance measurement, μ-FTIR, μ-Raman, SEM-EDX.	Mars red (in *Lady Santa Ana*).	Red ochre, yellow ochre, hematite.	Mars red is identified by the absence of minerals like calcite or clay. In addition, its IR band at 608–609 cm^{-1} is more intense than that of hematite.

Table 1. *Cont.*

Reference	Where the Pigments Come from?	Which Techniques Were Used?	Which Pigments Were Identified?	Are Ochres also Present?	Why Identified as Mars Pigment?
Franquelo, Perez-Rodriguez, 2016 [33]	Samples from various representative artworks of Southern Spain's Cultural Heritage, including Spanish Gothic and Andalusian Baroque polychrome sculptures, canvases, and altarpieces.	Optical microscopy, SEM-EDX, μ-Raman spectroscopy, μ-FTIR microscopy, Py-GC/MS.	Mars red.	Natural red, ochre.	Presence of Al, K, and S, coming from the synthesis of the Mars pigment.
Ionescu et al., 2004 [34]	Painting from Princely church of Curtea de Arges (1352–1377).	Optical microscopy, SEM-EDX, microchemical test,	Mars red.	Red earth, red ochre, yellow ochre.	XRF highlighted the presence of Fe, Ca, C, and S. Mars red was used in a documented restoration work.
Li et al., 2014 [35]	Wall paintings at Jokhang Monastery in Lhasa, Tibet, China, 1850–1900 (?).	XRF, PLM, Raman spectroscopy, SEM-EDX.	Mars red.	-	Iron detected by XRF.
Rizzo et al., 2002 [36]	*Sacred Family with Angels*, by Leonardo Glores, XVII century, Peru/South America. Tempera over canvas without varnish.	Spectrophotometer, TG-DSC.	Original painting: Mars red, yellow ochre; Restoration paints: Yellow ochre, Mars yellow, red ochre, Mars red.	Yellow ochre in the original painting and also used as pigment for the restoration work.	Not explained.
Sawczak et al., 2009 [37]	Wall paintings in the Little Christopher chamber of the Main Town Hall (Gdansk). Frescos 1400 and 1427.	Portable XRF, Raman.	Mars red, Mars yellow.	Red ochre, yellow ochre.	Not explained. The terms *ochre* and *Mars pigments* are used as synonymous.
Schenatto, Rizzuto, 2024 [38]	*Sessões da corte de Lisboa*, oil on canvas, 1922, and *Príncipe Dom Pedro e Jorge de Avirez a bordo da fragata União*, oil on canvas, 1922, both by Oscar Pereira da Silva.	Infrared reflectography, ED-XRF, Raman.	Mars red.	Yellow ochre.	Not explained.

Table 1. *Cont.*

Reference	Where the Pigments Come from?	Which Techniques Were Used?	Which Pigments Were Identified?	Are Ochres also Present?	Why Identified as Mars Pigment?
Townsend 1993 [11]	Pigments from palette of J.M.W Turner (1792–1850) and some paints: *Interior of a Gothic Church* (1797, wood) and *The Vision of Jacob's Ladder* (1800–1810, reworked c. 1830, painting on canvas).	Light and UV microscopy, microchemical test, thin-layer chromatography (TLC), EDX, XRD, FTIR.	Mars red, Mars orange, Mars yellow.	Yellow ochre.	The main difference between ochre and synthetic pigments lies in the particle size: Ochres vary due to natural mineral grinding, while synthetic pigments have uniform size. Turner used synthetic pigments throughout his career, as documented in the article.
Vermeulen 2022 [39]	Six impressionist and post-impressionist paintings of three leading Puerto Rican artists: Francisco Oller (1833–1917): *Trapiche meladero*, 1890, oil on canvas, and *Bodegón con guanábanas*, 1890, oil on wood, and *Bodegón con guanábanas y utensilios*, 1890–91, oil on canvas; José Cuchí y Arnau (1857–1925): *La Chula*, 1895, oil on canvas, and *Mujer en la playa*, 1897, oil on canvas; Ramón Frade (1875–1954): *Rêverie d'amour*, 1905, oil on wood.	MA-XRF, reflectance imaging spectroscopy (RIS), SEM-EDX, Raman spectroscopy, HPLC-DAD-ESI-Q-ToF.	Mars red.	Yellow ochre, red ochre.	Not explained.
Żmuda-Trzebiatowska et al., 2015 [40]	Original painting materials (paint tubes) of J. Matejko, XIX century.	Raman, XRF, SEM-EDX, LIPS, FTIR.	Mars red.	Yellow ochre.	Not explained.

Legenda: GC/MS = gas chromatography–mass spectrometry (Py-GC/MS = pyrolysis GC/MS); XRF = X-ray fluorescence; FTIR = Fourier-transform infrared spectroscopy; SEM-EDX = scanning electron microscopy with energy dispersive X-ray spectroscopy; PLM = polarized light microscopy; TG-DSC = thermogravimetric analysis and differential scanning calorimetry; LIPS = laser-induced plasma emission spectroscopy; MA-XRF = macro X-ray fluorescence; HPLC-DAD-ESI-Q-ToF = high-performance liquid chromatography–diode array detector–electrospray ionization–quadrupole–time of flight.

From the review of the articles shown in Table 1, it was first observed that the analytical techniques most used by the authors for element analyses were XRF, LIPS, and SEM-EDX. Optical microscopy and SEM (on polished sections, thin sections, or painted surfaces) were employed to investigate the morphology and possible stratigraphy of the painting layer. Raman spectroscopy and FTIR spectroscopy instead identified the molecular composition. References were also found for the use of TG-DSC and XRD for qualitative and quantitative analysis of molecules and detection of crystalline compounds, respectively. Microchemical tests and chromatographic techniques (GC-MS, Py-GC-MS, TLC, and HPLC-DAD-ESI-Q-ToF) were used for the study of binders.

Franquelo et al. [24] and Franquelo and Rodriguez [33] highlighted that the presence of minerals naturally associated with ochres (such as gypsum, kaolinite, calcite, etc.) could be a primary discriminator between natural and synthetic iron pigments, as Mars pigments contain fillers in much smaller quantities than ochres. According to the authors, the IR signal at 608–609 cm^{-1} can also be indicative, as it is more intense for Mars pigments than for hematite. Finally, the presence of elements or minerals related to the raw materials used to produce Mars pigments can be further proof of the type of pigment [16]. Townsend, 1993 [11], highlighted the importance of pigment grain size in differentiating the two materials. Ochres are obtained by grinding the extracted mineral, resulting in a wide range of particle sizes. In contrast, Mars pigments, obtained by synthesis, are characterized by a more uniform and fine particle size distribution.

Čukovska et al. [32] were unable to determine whether Dicho Zograph used ochres or Mars pigments in their studies but suggested the use of the Raman band at 660 cm^{-1} as a possible discriminator since it is not observed in Mars pigments but is common in ochres.

Regarding the use of the term, the present study first ensured that the possible presence of Mars pigments was consistent with their dissemination (late 18th century) [8,31] or that their presence in an earlier artwork was due to restoration interventions. This is the case with the *Sacred Family with Angels* (Leonardo Glores, 17th century, Peru) [36]. The presence of Mars pigments detected by the authors might be due to the restoration interventions the canvas underwent. The same was seen by Ionescu et al. [34], who found Mars red in a 13th-century painting, and by Franquelo et al. [24], where the same pigment was observed on a 14th-century polychrome sculpture. In both cases, the authors believed that Mars red was used during the restoration work.

3. Review of Commercial Mars Pigment and Ochre

To evaluate what is currently meant by the terms *ochre* and *Mars pigments*, the catalogs of various companies in the sector were consulted. For each Mars pigment, iron pigment, or ochre found, the technical data sheet and the safety data sheet were reviewed. Commercially available pigments are listed in Table 2.

To ensure the anonymity of the companies, the full names of the pigments are not included in Table 2, and only the description of the pigment class to which they belong is provided. Numbers were added to differentiate them. For this reason, many pigments are listed with the same name but different declared compositions. If a company classified a synthetic iron oxide as ochre, the term “ochre” was retained. Companies typically name materials according to their class (yellow iron oxide, yellow ochre, Mars pigment, etc.), and they often add specific color characteristics, such as brightness, hue, or particle size, to differentiate them.

Many of the pigments studied share the same name (or a very similar name) and a similarly declared composition. The differences between these materials could be due to variations in particle size or slight color differences caused by the possible presence of additives not listed in the technical and safety data sheets. Natural ochres and earth pigments are in fact characterized by a certain variability in composition, which may not always be disclosed by the manufacturer.

Table 2. List of the found commercial Mars pigment and ochres. The capital letter preceding the name of the pigment is the acronym chosen to indicate the company that produces it.

Pigment	Color	Information Available
A—Iron Oxide Yellow 1	Yellow	Synthetic iron hydroxide. Pigment Yellow 42.77492, α-FeO(OH)
A—Iron Oxide Yellow 2	Yellow	Pigment Yellow 42, C.I. 77492, α-FeOOH
A—Iron Oxide Yellow 3	Yellow	α-FeO(OH). Pigment Yellow 42, C.I. 77492
A—Iron Oxide Yellow 4	Yellow	C.I. Pigment Yellow 42.77492 (FeOOH) (CAS No. 20344-49-4), C.I. Pigment Red 101.77491 (Fe_2O_3) (CAS No. 1309-37-1)
A—Iron Oxide Yellow 5	Yellow	α-FeO(OH). Pigment Yellow 42, C.I. 77492
A—Iron Oxide Yellow 6	Yellow	Pigment Yellow 43, C.I. 77491 Fe_2O_3 + Al_2O_3 + Mn_2O_3 + SiO_4 + $CaCO_3$. Natural product
A—Iron Oxide Yellow-Orange	Orange	FeO(OH); Pigment Yellow 42, C.I. 77492. Synthetic iron oxide gamma-FeOOH
A—Iron Oxide Orange	Orange	Mixture of Pigment Yellow 42.77492 (FeO(OH)) and Pigment Red 101.77491 (Fe_2O_3)
A—Iron Oxide Red 1	Red	Synthetic Iron oxide α-Fe_2O_3. Pigment Red 101, C.I. 77491
A—Iron Oxide Red 2	Red	Synthetic Iron oxide α-Fe_2O_3. Pigment Red 101, C.I. 77491
A—Iron Oxide Red 3	Red	Synthetic Iron oxide α-Fe_2O_3. Pigment Red 101, C.I. 77491
A—Iron Oxide Red 4	Red	Synthetic Iron oxide α-Fe_2O_3. Pigment Red 101, C.I. 77491
A—Iron Oxide Red 5	Red	Synthetic Iron oxide α-Fe_2O_3. Pigment Red 101, C.I. 77491
A—Iron Oxide Red 6	Red	Synthetic Iron oxide α-Fe_2O_3. Pigment Red 101, C.I. 77491
A—Caput Mortuum Synthetic	Red	Synthetic Iron oxide α-Fe_2O_3. Pigment Red 101, C.I. 77491
A—Iron Oxide Red 7	Red	Fe_2O_3. Pigment Red 101, C.I. 77491
A—Iron Oxide Red	Red	Synthetic Iron oxide α-Fe_2O_3. Pigment Red 101, C.I. 77491
A—Yellow Ochre, 1	Yellow	Pigment Yellow 43, C.I. 77492. Natural product
A—Yellow Ochre 2	Yellow	Natural yellow earth, Pigment Yellow 43, C.I. 77492
A—Yellow Ochre 3	Yellow	Natural yellow earth, Pigment Yellow 43, C.I. 77492
A—Yellow Ochre 4	Yellow	Natural yellow earth from France. SiO_2 + Al_2O_3 + Fe_2O_3. Pigment Yellow 43, C.I. 77492
A—Yellow Ochre 5	Yellow	Natural yellow earth from France: Kaolin + Goethite. SiO_2 + Al_2O_3 + Fe_2O_3. Pigment Yellow 43, C.I. 77492
A—Yellow ochre 6	Yellow (orange)	Natural yellow earth from France. SiO_2 + Al_2O_3 + Fe_2O_3. Pigment Red 102, C.I. 77491
A—Yellow Ochre 7	Yellow	Natural ochre from Italy. Pigment Yellow 43, C.I. 77492
A—Yellow Ochre 8	Yellow	Natural yellow ochre; Pigment Yellow 43, C.I. 77492
A—Yellow Ochre 9	Yellow	Natural ochre from Italy. Pigment Yellow 43, C.I. 77492
A—Yellow Ochre 10	Yellow	Pigment Yellow 43, C.I. 77492 Mixture of natural barium sulfate ($BaSO_4$), earth containing iron oxide (Fe_2O_3 + MnO_2 + SiO_2), and iron oxide yellow (FeO(OH))
A—Red Ochre 1	Red	Pigment Red 102, C.I. 77491. Natural product
A—Red Ochre 2	Red	Pigment Red 102, C.I. 77491
A—Red Ochre 3	Red	Natural red earth from Spain; Pigment Red 102, C.I. 77491
A—Orange Ochre 1	Yellow (orange)	Natural yellow earth from France. Pigment Yellow 43 (C.I. 77492) and Pigment Red 102 (C.I. 77491)
A—Orange Ochre 2	Orange	Natural earth from France. SiO_2 + Al_2O_3 + Fe_2O_3 + Fe_3O_4. Pigment Yellow 43 + Pigment Red 102 + Pigment Black 11
A—Gold Ochre 1	Yellow	Mixture of calcium carbonate and synthetic iron oxide. Pigment Yellow 42, C.I. 77492
A—Gold Ochre 2	Yellow	Natural yellow ochre from Italy. Pigment Yellow 43, C.I. No. 77492
B—Yellow Ochre 1	Yellow	ND
B—Yellow Ochre 2	Yellow	ND
B—Yellow Ochre 3	Yellow	Natural earth pigment derived from iron-rich clay deposits that are present all over the world; this Yellow Ochre comes from the hilly regions around Verona, Italy
B—Golden Ochre	Yellow	Natural Iron Oxides
B—Orange Ochre 1	Orange	A rich orange pigment collected from the banks of the river Fleet in London
B—Pink Ochre 1	Pink	ND
B—Red Ochre	Red	Synthetic Iron Oxides
B—Red Pigment 1	Red	Synthetic Iron Oxides.

Table 2. *Cont.*

Pigment	Color	Information Available
B—Red Pigment 2	Red	Natural earth pigment that was originally found in the volcanic areas in Pozzuoli, Italy
B—Red Pigment	Red	Iron oxide and chalk
B—Mars Red Pigment	Red	Synthetic Iron Oxides
B—Red Oxide Pigment	Red	Artificial mineral pigment, hydrated ferric oxides
B—Mars Yellow Pigment	Yellow	Synthetic Iron Oxides
B—Yellow Oxide Pigment	Yellow	Artificial mineral pigment, hydrated ferric oxides
B—Orange Oxide	Orange	Artificial mineral pigment, hydrated ferric oxides
C—Mars orange	Orange	Synthetic iron oxide—PY42—77492—inorganic
C—Mars yellow	Yellow	Synthetic iron oxide—PY42—77492—inorganic
C—Mars red	Yellow	Synthetic iron oxide—PR101—77491—inorganic
C—Yellow ochre 1	Yellow	Synthetic iron oxide—PY43—77492—inorganic
C—Yellow ochre 2	Yellow	Synthetic iron oxide—PY43—77492—inorganic
C—Yellow ochre 3	Yellow	Synthetic iron oxide—PY43—77492—inorganic, Synthetic iron oxide—PY42—77492—inorganic, Zinc oxide—PW4—77947—inorganic
C—Gold ochre	Yellow	Natural iron oxide—PY43—77492—inorganic
C—Red ochre 1	Red	Natural iron oxide—PY43—77492—inorganic
C—Gold 1	Yellow	Mica+ Synthetic iron oxide—PW20—77019—inorganic
C—Gold 2	Yellow	Mica+ Synthetic iron oxide—PW20—77019—inorganic
C—Gold 3	Yellow	Mica+ Synthetic iron oxide—PW20—77019—inorganic
C—Bronze 1	Yellow	Mica+ Synthetic iron oxide—PW20—77019—inorganic, Carbon black—PBk7—77266—inorganic
C—Bronze 2	Yellow	Mica+ Synthetic iron oxide—PW20—77019—inorganic, Carbon black—PBk7—77266—inorganic
D—Yellow ochre 1	Yellow	Natural earth of a slightly transparent warm yellow. PY43
D—Yellow ochre 2	Yellow	Or Chrome Yellow Rutile, is a slightly ochre yellow-orange. Synthetic. Chromium antimony titanium rutile. PBr24
D—Gold ochre	Yellow	Or Yellow of Rome, is a zinc ferrite. Synthetic. PY119
D—Red ochre	Red	Obtained by calcination of yellow ochre. PR102
D—Ocre de Ru	ND	Reconstituted color shade based on natural earth and synthetic pigment. Natural earth + phthalocyanine green. PBr7, PG7
D—Mars yellow	Yellow	Azo pigment and natural earth. In other times, this pigment was made from a concentrate of animal urine from the Indies. Py1, PBr7
D—Mars red	Red	Synthetic iron oxide. Very dark red-brown. PR101
D—Red pigment	Red	Synthetic iron oxide
E—Yellow ochre 1	Yellow	Natural earth
E—Yellow ochre 2	Yellow	Natural earth
E—Yellow ochre 3	Yellow	Natural earth
E—Yellow ochre 4	Yellow	Natural earth
E—Yellow ochre 5	Yellow	Natural earth
E—Yellow ochre 6	Yellow	Natural earth
E—Gold ochre 1	Yellow	Natural earth
E—Gold ochre 2	Yellow	Natural earth
E—Orange ochre	Orange	Natural earth
E—Red ochre 1	Red	Natural earth
E—Red ochre 2	Red	Natural earth
E—Hematite 1	Red	Natural earth
E—Hematite 2	Red	Natural iron oxide (Group 2)
E—Red bole 1	Red	Natural earth
E—Red bole 2	Red	Mixture of coloring earths
E—Red pigment 1	Red	Mix of natural earth
E—Red pigment 2	Red	Mix of natural earth
E—Red pigment 3	Red	Mix of natural earth
E—Red pigment 4	Red	Natural iron oxide (Group: 5)
E—Red pigment 5	Red	Mixture of coloring earths
E—Red pigment 6	Red	Iron oxide (Group: 2)
E—Mars yellow	Yellow	Iron oxide (Group: 1)
E—Mars orange	Orange	Iron oxide (Group: 1)
E—Mars red	Red	Iron oxide (Group: 1)

From the study of iron pigments marketed by companies, it was observed that the trade name does not always coincide with what the pigment should be.

A pigment called red ochre was found to be made from synthetic iron oxides (B—Red ochre). One yellow ochre, according to the data sheets, is composed of chromium antimony titanium rutile (D—Yellow ochre 2), one golden ochre is composed of synthetic zinc ferrite (D—Gold ochre), and finally, one Mars yellow was found to be composed not of synthetic iron oxides but of an azo pigment and natural earth (D—Mars yellow). In some cases, companies reported the addition of other pigments to change the color gradation. Ochres containing natural iron oxides to which are added synthetic iron oxides and zinc oxides, mica, carbon black, or phthalocyanine green were also found. Finally, a red ochre obtained by calcining yellow ochre was found commercially (D—Red ochre); it would thus be an artificial pigment. The addition of any extenders such as barite or calcite was never declared.

In general, consistency between the trade name of the material and its composition was observed for most pigments. However, cases of great difference between the trade name and the chemical composition were also observed. Powder pigments are widely used as conservation materials for historical artifacts. In cases where the trade name does not match the pigment content, this could be a problem. The use of materials that are not philologically correct and not compatible with historic materials increases the risk of unpredictable degradation reactions.

4. Experimental Part

The possibility of differentiating Mars pigments from natural ochres was investigated using external reflection infrared spectroscopy (FTIR-ER) both on different samples of Mars yellow and red in powder form and on fragments of red ochre and yellow ochre. In parallel, paint layers on paper, one with Mars yellow and another one with yellow ochre, were studied to see if it is possible to differentiate the samples when applied to a surface. The paint layers were prepared in the laboratory 10 years ago, thus showing natural aging of the binder, whose expected duration can range from a few months [41–44] to years [45]. In addition, the paper substrate allowed for noninvasive analysis using FTIR-ATR spectroscopy, which is generally destructive. Previous analyses did in fact show that the mode of analysis did not irreversibly damage the specimen. Thus, the results obtained by a relatively recent technique such FTIR-ER could be compared with those obtained by an established one.

FTIR-ER is increasingly used in the field of cultural heritage because it is portable, noninvasive, and has a wide acquisition range (375–7500 cm^{-1}) [23,46–48], and it has also found wide use in the characterization of archaeological objects [49–51]. The instrument can provide many indications of surface molecular composition. The main difficulty with the technique is the interpretation of the spectra due to the complexity and variability of pigment and binder mixtures and surface morphology. This difficulty is due to the nature of the technique, which combines different types of reflection and leads to spectral distortions that are absent in more traditional techniques. This mode of IR analysis was chosen to assess its potential in distinguishing ochres from Mars pigments on real artworks since noninvasive techniques are increasingly preferred over traditional ones to investigate archaeological objects that are too valuable or in such a critical state of preservation that they do not even allow the collection of micro-fragments to perform the analysis.

The FTIR-ATR technique, which is also based on a reflection phenomenon, has long been employed in the field of cultural heritage and, more specifically, in archaeology [51–53]. Its acquisition range varies depending on the type of crystal used, though it is generally limited to the mid-IR region. The spectra obtained with this method are simpler compared to those from FTIR-ER, as they typically do not present distortions and closely resemble the spectra produced by traditional transmission infrared spectroscopy. However, unlike FTIR-ER, this technique requires the collection of at least a small sample, which must be placed in close contact with the analysis crystal by applying pressure to achieve high-quality spectra.

This method is therefore unsuitable for archaeological objects from which samples cannot be taken or for materials that are too fragile to withstand the applied pressure without damage. Compared to FTIR-ER, FTIR-ATR generally allows for more superficial analyses without probing deeper layers and is better suited to rough and uneven surfaces, which pose greater challenges for radiation reflection.

4.1. Materials and Methods

4.1.1. Materials

To carry out FTIR-ER analysis of the Mars pigments provided by Kremer Pigmente [54], anhydrous KBr and the pigment under investigation were ground and mixed in an agate mortar and pressed. The resulting mixture was subjected to the action of a press until a thin pellet was obtained. The pellet was deposited on a stand and placed in front of the analysis window.

The paint layers were prepared on Fabriano [55] cotton paper, using Zecchi [56] pigments and bleached crude linseed oil as a binder.

As for the analysis of raw materials and pictorial layers on paper, it was sufficient to place the material subject of study in front of the window. For FTIR-ATR analysis, the paint layers on paper were placed in close contact with the analysis crystal by applying gentle pressure. Table 3 shows the materials analyzed.

Table 3. Materials analyzed in experimental part.

Powder Pigments and Raw Materials Characterized by FTIR-ER			
Yellow Pigments		**Red Pigments**	
Pigment	**Description**	**Pigment**	**Description**
MY1: Iron Oxide Yellow, maize yellow, #48001	Synthetic iron oxide	MR1: Iron Oxide Red 110 M, light, #48100	Red pigment 101.77491 Fe_2O_3
MY2: Iron Oxide Yellow 415, greenish, #48020	Yellow pigment 42 (FeOOH)	MR2: Iron Oxide Red 120 M, #48120	Red pigment 101.77491 Fe_2O_3
MY3: Iron Oxide Yellow 940, dark, #48040	C.I. Yellow pigment 42.77492 (FeOOH) red pigment 101.77491 (Fe_2O_3)	MR3: Iron Oxide Red 130 B, medium, #48150	Red pigment 101.77491 Fe_2O_3
MY4: Iron Oxide Yellow 930, dark, #48045	Yellow pigment 42.77492, FeO(OH)	MR4: Iron Oxide Red, clinker red, #48151	Red pigment 101.77491 Fe_2O_3
MY5: Iron Oxide Yellow, maize yellow, #48001	Iron oxide pigment synthetic	MR5: Iron Oxide Red 130 M, medium, #48200	Red pigment 101.77491 Fe_2O_3
MY5: Iron Oxide Yellow-Orange 943, Gamma, #48050	FeO(OH); yellow pigment 42.77492	MR6: Iron Oxide Red 160 M, #48210	Red pigment 101.77491 Fe_2O_3
		MR7: Caput Mortuum Synthetic 180 M, #48220	Red pigment 101.77491 Fe_2O_3
		MR8: Iron Oxide Red 222, dark, #48250	Red pigment 101.77491 Fe_2O_3
		MR9: Iron Oxide Red, micronized, #48289	Iron oxide (II), 98–100%
Raw materials			
YO1: Yellow Moroccan ochre, in pieces, #1164205	Raw materials such as minerals and earth	RO1: Red Moroccan ochre, in pieces, #12450	Red ochre
		RO2: Red bole in pieces, #40520	Natural mixture of hematite, quartz, and feldspars.
Characterized paper pictorial layers via FTIR-ATR and FTIR-ER			
MYP: Mars yellow in oil on paper		YOP: Yellow ochre in oil on paper	

Figure 1 shows optical microscope images of the two pictorial layers on paper. The images made it possible to observe the effect of the presence of oil on the surface appearance and the different color tone.

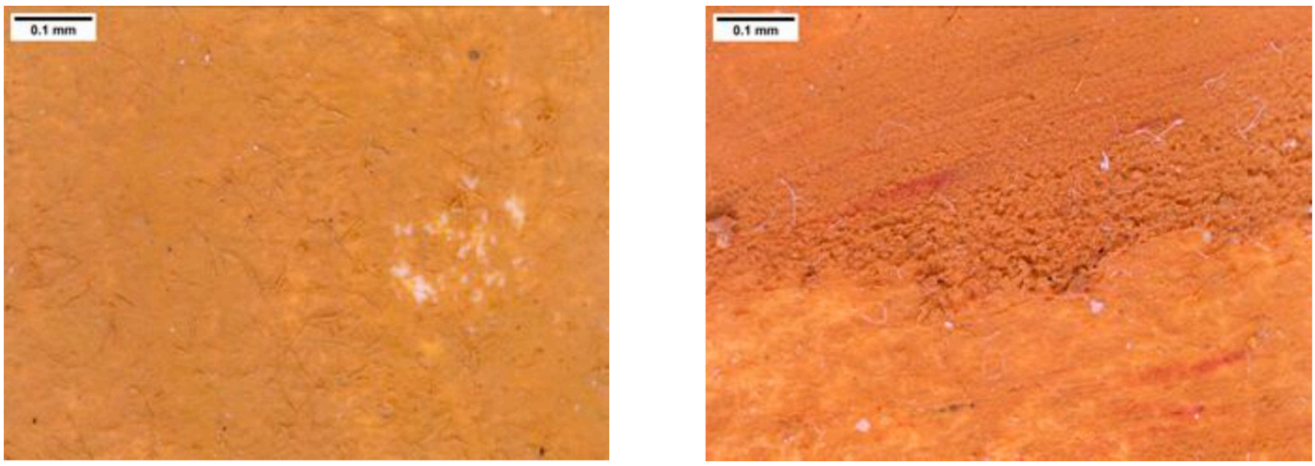

(**a**) (**b**)

Figure 1. Light microscope image of MYP (**a**) and YOP (**b**). The images show the morphology of the pigments when oil is used as a binder and their chromatic gradation.

4.1.2. Methods

Pigment powders and raw materials were studied by external reflection infrared spectroscopy (FTIR-ER). A Bruker Alpha FTIR instrument with total external reflection module and DTGS detector (spectral range: 7500–375 cm^{-1}; resolution: 4 cm^{-1}; scans: 200) was used. The spectra were then edited with OPUS software (version 7.2).

Pictorial layers on paper were characterized by comparing spectra obtained by FTIR-ER and by FTIR-ATR. A Thermo Scientific Nicolet iS10 FTIR instrument in ATR (Attenuated Total Reflection) mode with diamond crystal (spectral range: 4000–600 cm^{-1}; resolution: 4 cm^{-1}; scans: 32) was used for this purpose. The spectra were then edited with Omnic software (version 8.3.103).

FTIR-ER spectra, as previously discussed, can be difficult to interpret due to distortions or inversions in the shape of the bands and absorption frequencies. This complexity was particularly evident in paint layers on paper, where the combination of support, pigments, and binder complicated the spectra. FTIR-ATR analysis of the same areas facilitated the interpretation. In contrast, this approach was not necessary for the characterization of powder pigments, where the presence of a single component made the spectra significantly easier to interpret.

Samples on paper were observed with a Maozua USB001 MicroCapture Plus handheld digital microscope.

4.2. Results

4.2.1. Characterization of Raw Materials

Mars Yellow and Yellow Ochre

Figure 2 shows the FTIR-ER spectra of Mars yellow powder and yellow ochre—raw material.

From an initial observation of the FTIR-ER spectra of the analyzed materials, the presence of accessory minerals in the ochres was immediately clear, as the spectra of the ochres showed many more signals than the Mars pigments.

The IR band at about 3100 cm^{-1} observed in all MY spectra is associated with the Fe^{2+}-OH vibration of goethite [57–59]. The other characteristic peaks of goethite observed in all spectra of MY were between 1660 and 1614 cm^{-1} (bending of hydroxyl groups [57,60,61]), at about 900 and 795 cm^{-1} (vibrational deformation of Fe^{2+}-OH bond [57,60,61]), and, finally, Fe-O stretching at 460 cm^{-1} [28,57,60]. The signal at 670 cm^{-1}, which is also characteristic of goethite [60], was observed only in the spectrum of MY2 and MY3. In MY5 the peaks at about 900 and 795 cm^{-1} were not very intense. In contrast, peaks characteristic of lepidocrocite fell at 1150, 1021, 754, and 616 cm^{-1}[62–65]. These signals, all more or less intense, were observed in all FTIR-ER spectra of Mars pigments. MY5 is the only

pigment to show all four very intense bands, consistent with what is described in the data sheet provided by the manufacturers, which states the use of lepidocrocite to produce the pigment. The peaks at 1150 and 616 cm^{-1} were also observed in the spectra of MY3 and MY4. The peak at 1021 cm^{-1} was seen in all spectra of MY. Patterns characteristic of calcite (1431 and 875 cm^{-1} [22]) in MY3 and barite (981 and 613 cm^{-1} [28]) in MY3 and MY4, which were probably added as fillers, were observed.

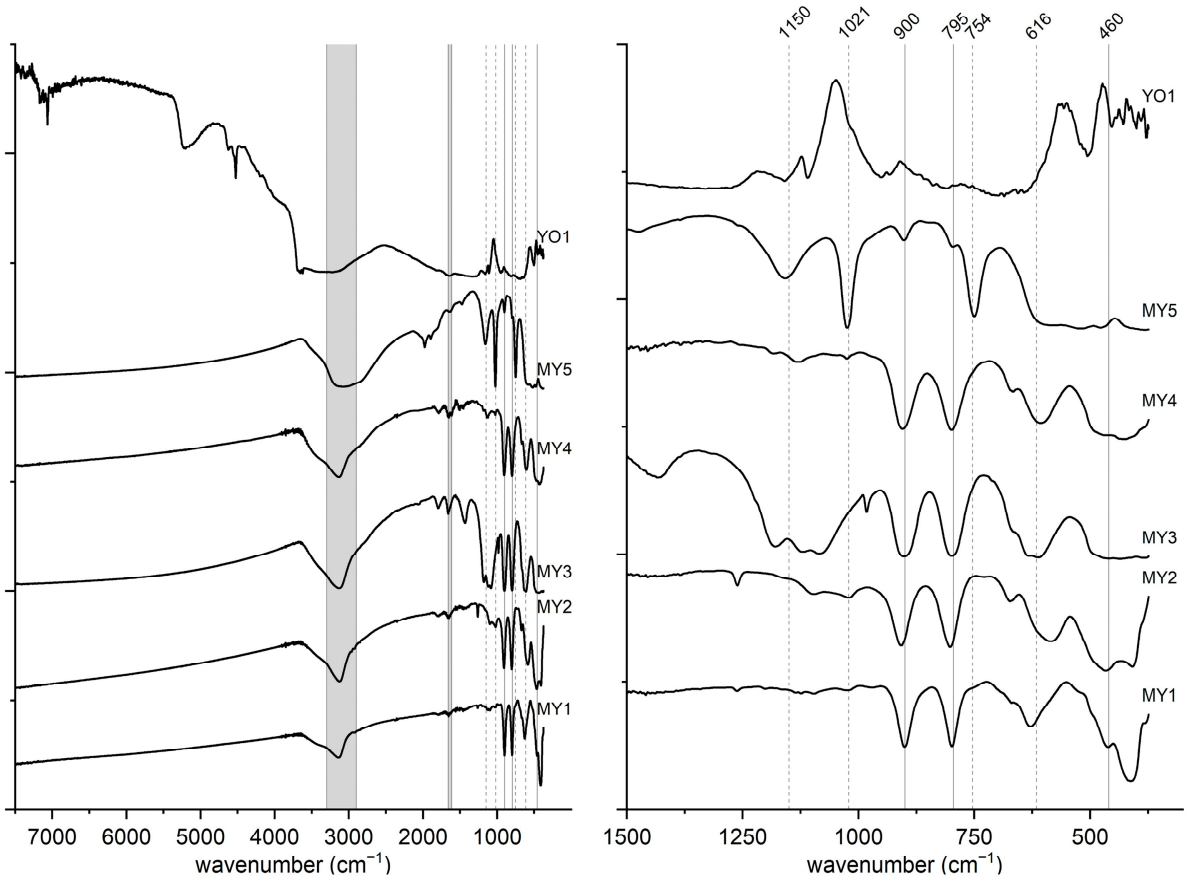

Figure 2. FTIR-ER spectra of yellow pigments. Gray-filled areas mark regions containing the most prominent signals for identifying goethite. Solid lines represent goethite's primary peaks, while dashed lines indicate lepidocrocite's characteristic peaks.

From the observation of yellow ochre in the form of raw material (YO1), the presence of signals in the overtones region (4000–7500 cm^{-1}) absent in the spectra of MY was first observed. These bands were attributed to kaolinite [66,67] (7168, 7111, 7963, and 4527 cm^{-1}). Between 4000 and 500 cm^{-1}, peaks due to combinations of stretching and bending or overtones of iron oxides were observed [66,68], which have never been observed in Mars pigments. The presence of kaolinite was also confirmed by peaks at 3650, 3624, 3433, 1130 (inverted), 1050 (inverted), 911 (inverted), and 704 cm^{-1} [62]. The inverted FTIR-ER signals are due to a spectral distortion typical of the technique. The band at 3100 cm^{-1} of iron oxyhydroxide is not clearly distinguishable from the OH stretches of kaolinite, but the bending of the hydroxyl group at 1647 cm^{-1} characteristic of goethite remains visible. Of the characteristic doublet of α-FeOOH, the signal at 795 cm^{-1} (inverted) is still clearly distinguishable, while the peak at 900 cm^{-1} is partially hidden by kaolinite, so a shoulder can be observed, probably identifiable as this characteristic peak. Finally, the two peaks related to Fe-O stretching at 670 and 460 cm^{-1} are clearly observable. The lepidocrocite characteristic peaks, present in all Mars yellows to a greater or lesser extent, are not present in the FTIR-ER spectrum of ochre. The signal at 1333 cm^{-1} could be attributed to the presence of barite.

Mars Red and Red Ochre

Figure 3 shows the FTIR-ER spectra of powdered Mars reds and red ochres—raw material.

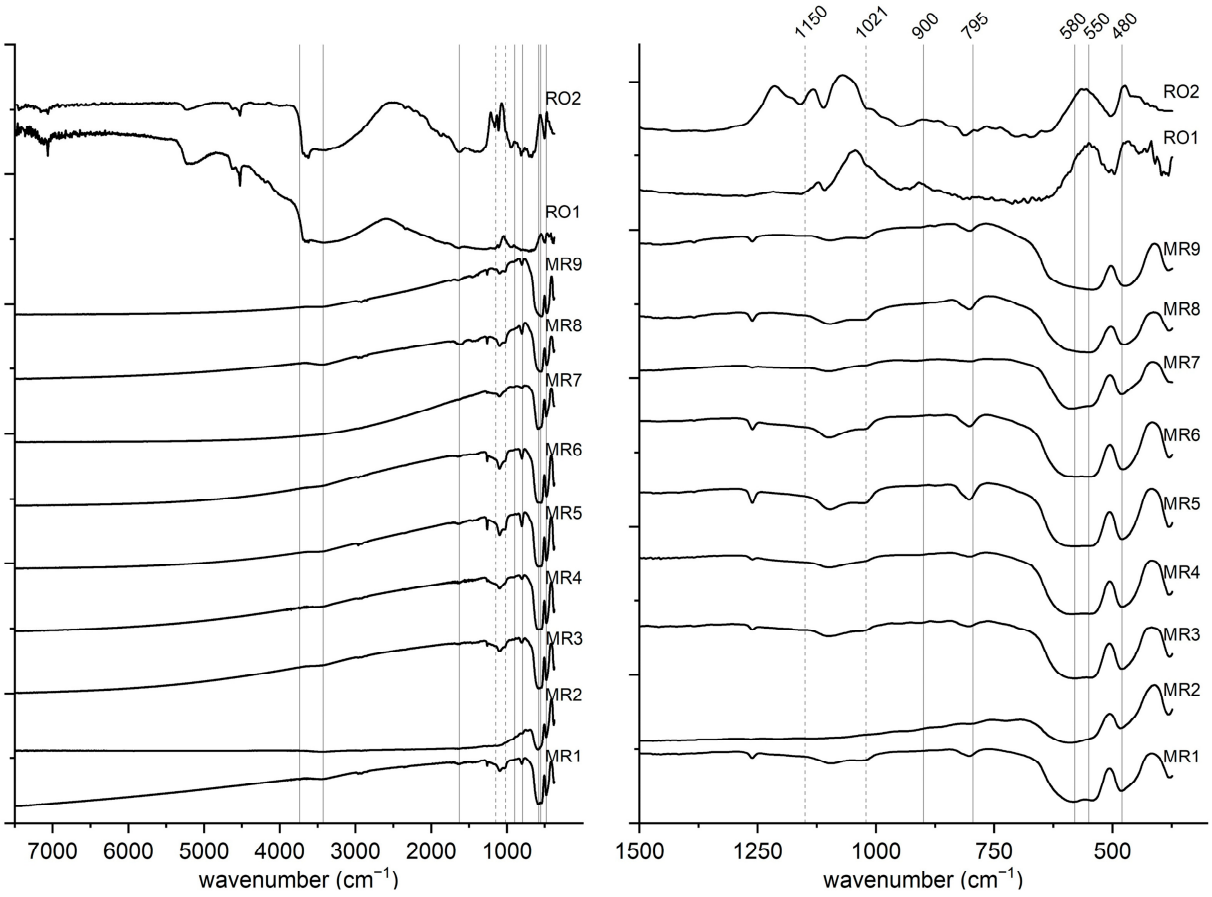

Figure 3. FTIR-ER spectra of red pigments. The solid lines indicate the hematite, goethite, and maghemite major peaks, and the dashed lines indicate the signals of lepidocrocite.

The FTIR-ER spectra show, as a first difference, the presence of many more signals in the ochre spectrum than in the spectra of the Mars pigments, indicating the presence of accessory minerals.

In all FTIR-ER spectra of MR, except for MR3, a weak band was observed at about 3740 cm^{-1}, which was absent in the two characterized red ochres. The peak represents the OH stretching of the maghemite [69,70]. The very broad signal at about 3430 cm^{-1} is due to the presence of hydroxyl groups. Some of the characteristic peaks of goethite (900 and 795 cm^{-1}) and lepidocrocite (1150 and 1021 cm^{-1}) have been found in all MR, while the peaks at 670 and 460 cm^{-1} for goethite and 754 and 616 cm^{-1} for lepidocrocite have never been observed. The signal at 1660 cm^{-1} seen in the goethite spectra shifted to lower values in the MR, at about 1630 cm^{-1}. Its presence is always related to the bending of goethite hydroxyl groups [70]. Three very intense peaks have always been observed in the FTIR spectra of the MR: a doublet at about 580 and 550 cm^{-1} and a single signal at 481/479 cm^{-1}. The peaks at 550 and 480 cm^{-1} are due to structural vibrations of hematite [62,71–73]. The peak at about 580 cm^{-1} could be due to stretching of the maghemite [62]. Another signal characteristic of hematite fell at 643 cm^{-1} [62] but was not observed in any spectrum. In all samples except MR4 and MR5, peaks were seen that could be attributed to the addition of carbonates such as calcite (1415 cm^{-1} [22]).

Also, in the case of the red ochres, the presence of kaolinite was observed due to its characteristic signals between 3600 and 3400 cm^{-1} and the overtones listed above. In RO1, the characteristic peaks of hematite at 559 and 473 cm^{-1} (both inverted) are clearly

distinguishable, and the absorbance at 643 cm^{-1}, which is absent in the IR spectra of Mars reds, was also observed. The bands indicating the presence of goethite clearly observed in the spectrum are at 1630, 897, and 810 cm^{-1}. Peaks characteristic of lepidocrocite and maghemite were not found. Thus, the RO1 pigment appears to be composed of hematite, goethite, kaolinite, and quartz (plus other silicates and aluminates not clearly identifiable).

As for RO2, characteristic signals of hematite were observed at 642, 559, and 480 cm^{-1}, while the peak at 580 cm^{-1} of maghemite is absent. Again, typical goethite peaks were present, although they are much less intense than in RO1, at 904 and 791 cm^{-1}. In addition to iron oxides, kaolinite, quartz, and, in this case, also a carbonate (probably calcite) were present.

4.2.2. Characterization of Pictorial Layers

The FTIR spectra (ATR and External Reflection modality) of the two pictorial layers on paper are shown in Figures 4 and 5.

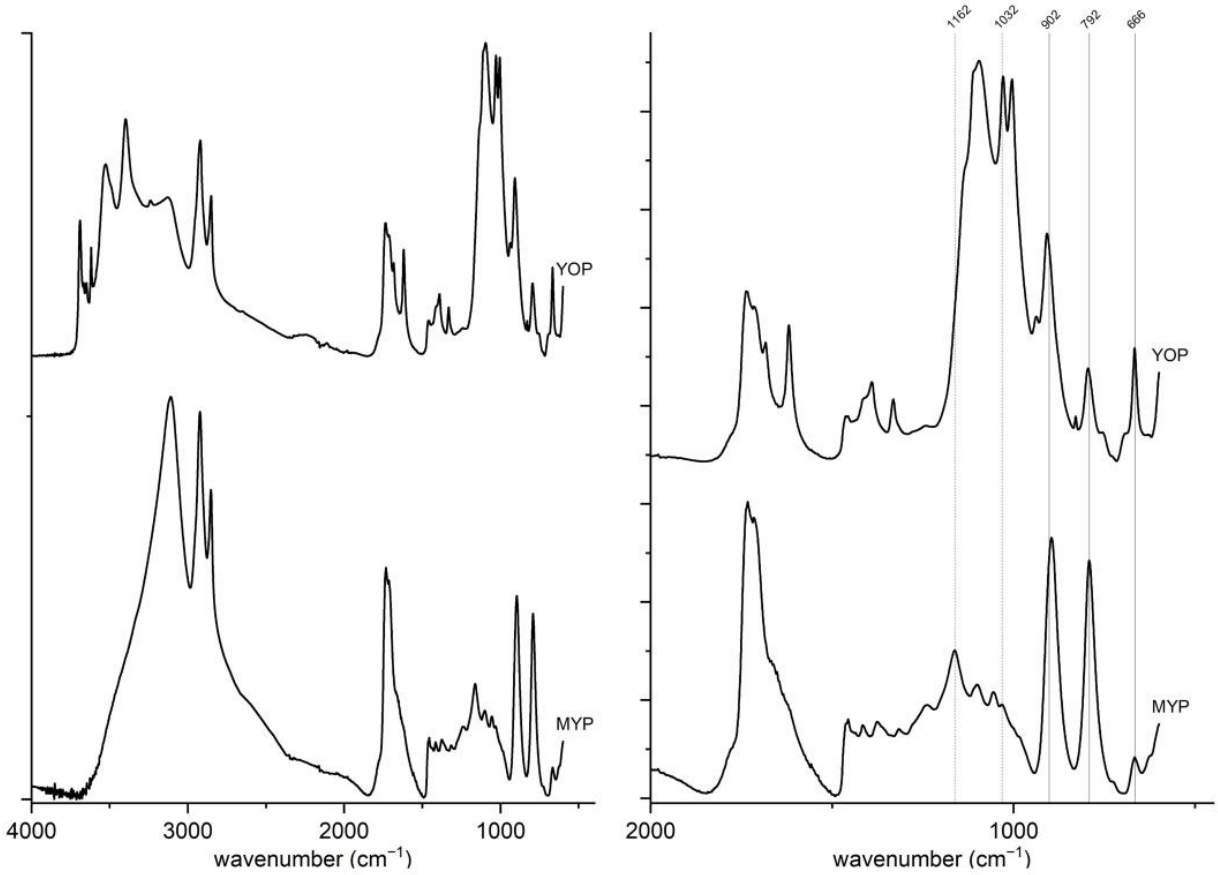

Figure 4. FTIR-ATR spectra of MYP and YOP. Solid lines represent goethite's primary peaks, while dashed lines indicate lepidocrocite's characteristic peaks.

Starting from the MYP spectra, the FTIR-ATR signals attributable to goethite are at 1662, 902, 792, and 666 cm^{-1} (Figure 4), while the FTIR-ER peaks are at 1647 (gray band), 924, 820, and 670 cm^{-1} (Figure 5). The characteristic peaks of lepidocrocite at 1162 and 1032 cm^{-1} (FTIR-ATR) and 1040 cm^{-1} (FTIR-ER) are also clearly observable. The other bands were attributed to the binder [47] and paper [48,74]. For yellow ochre (YOP), ATR signals at 908, 795, and 664 cm^{-1} (reflection mode at 1629, 894 and 443 cm^{-1}) were attributed to goethite (Figure 4). The characteristic bands of hematite were also seen at 634 cm^{-1} (in ATR) and 578 and 630 cm^{-1} (in FTIR-ER) (Figure 5). In addition to the chromophore peaks attributable to the presence of kaolinite, gypsum and quartz were observed.

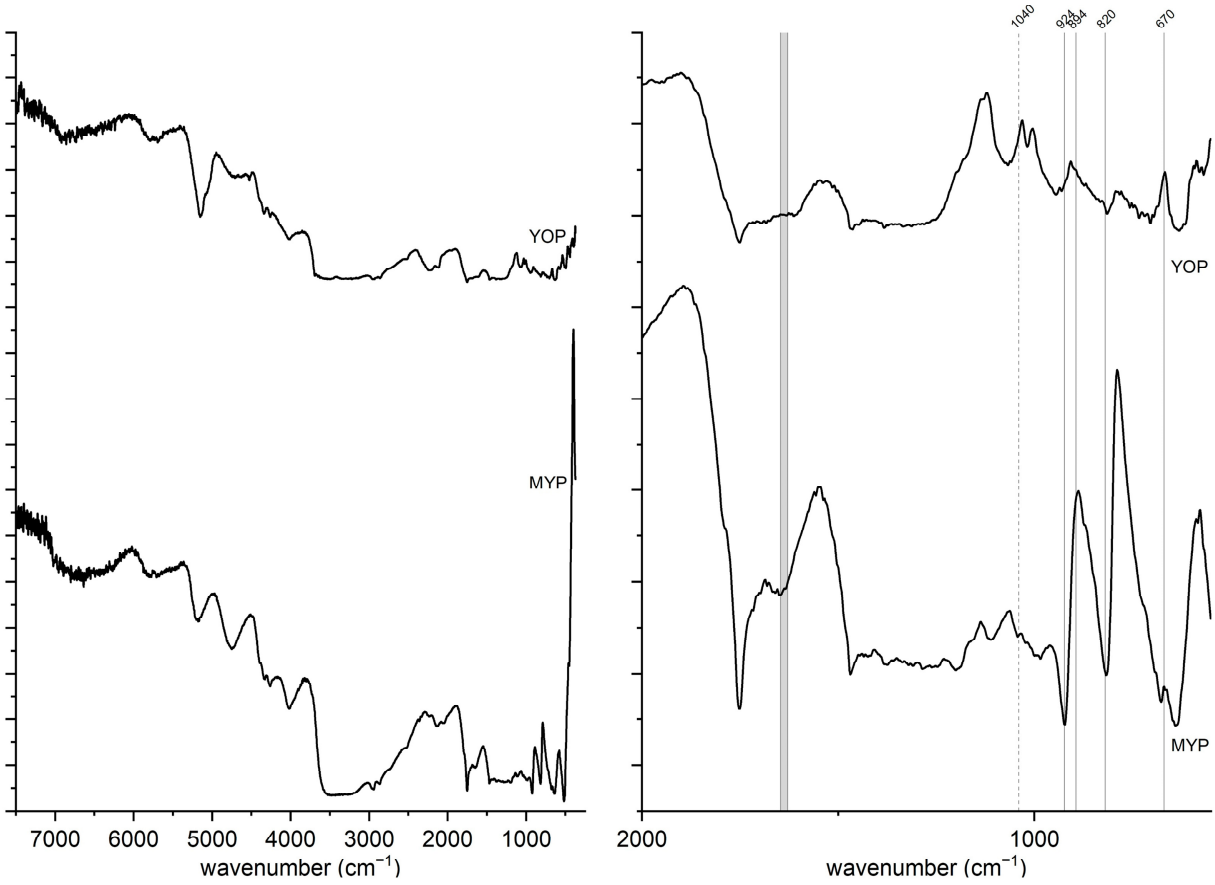

Figure 5. FTIR-ER spectra of MYP and YOP. Gray-filled areas mark regions containing the most prominent signals for identifying goethite. Solid lines represent goethite's primary peaks, while dashed lines indicate lepidocrocite's characteristic peaks.

The present study revealed that yellow ochres differ from MY in terms of the presence of accessory minerals and the absence of characteristic indicators of lepidocrocite. Although the natural presence of lepidocrocite in ochres is widely mentioned in the literature, no references were found among the studies identifying the mineral in the characterization of natural ochres. In addition, in ochres, it is more common to find the presence of accessory minerals, which are present in lower amounts in Mars pigments. Finally, the presence of hematite in ochres was observed, which is absent in MY because it is obtained by firing goethite. The presence of hematite, a mineral that can be found naturally associated with goethite in ochres, could be the means of distinguishing synthetic from natural iron yellows.

As for red pigments, in contrast to the barite found predominantly in MY, goethite, lepidocrocite, maghemite, and hematite were almost always found in this group of pigments, unlike in the red ochres, where the chromophores present were solely goethite and hematite.

5. Conclusions

This study aimed to evaluate methods for recognizing ochres and Mars pigments in works of art. Regarding the use of the terms, great confusion has been observed in the literature, as very often, the term Mars pigment is used as a synonym for ochre. The review of pigments on the market showed that the trade name did not always coincide with what the pigment should be, replicating the confusion of terms that emerged from the literature.

The literature review highlighted different ways of distinction between natural and synthetic iron pigments, in many cases on restored surfaces. The presence of accessory minerals is the most-discussed way. Another indicative characteristic is the morphology of

pigment grains. By Raman spectroscopy, it seems to be possible to differentiate pigments by observing some characteristic bands.

Finally, the experimental part showed that it might be possible to distinguish ochres from Mars pigments with FTIR-ER spectroscopy, too. The presence of accessory minerals in high concentrations and of different types could indicate that the pigment is an ochre. Another way of distinction is the presence of hematite in yellow ochres, which is absent in MY. In contrast, goethite was found in both MR and red ochres. Finally, a peak, at 642–643 cm^{-1}, assigned to the hematite that is absent in Mars reds, was observed from the study of red ochres. It is possible to study this issue further by analyzing more red ochres and MR to define whether this could be significant in differentiating the two pigments by FTIR-ER, which has the advantage of being portable and noninvasive and thus can be used with fragile objects or directly at archaeological sites.

The differentiation between Mars pigments and ochres therefore is very complex, but there are some details that seem to make it possible. Techniques such as FTIR-ER have shown some differences between the two types of pigments, and the literature has shown that even with other techniques, it is possible to differentiate the materials either by study of grain size or by observation of chemical composition.

In the future, this study could be further developed by expanding the analytical techniques used for the experimental part or by using chemometric methods such as PCA to further investigate the differentiation.

A schematic description of the results of the evaluation proposed in this study is presented in Figure 6.

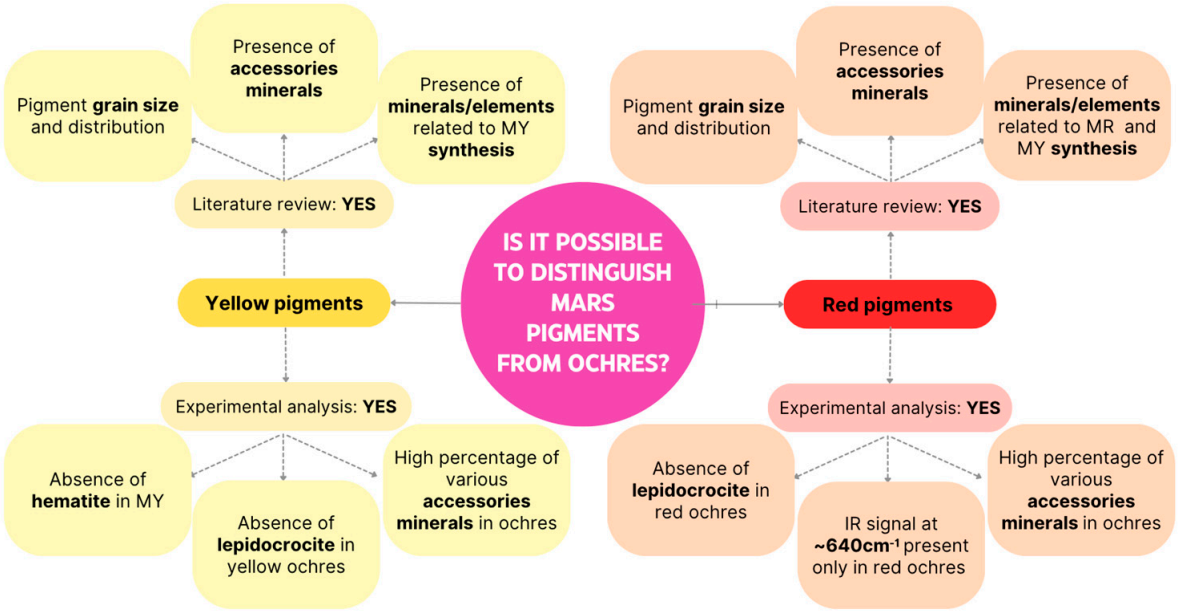

Figure 6. Schematic representation of the findings.

Author Contributions: Conceptualization, L.R.; methodology, L.R.; validation, C.C. and L.R.; formal analysis, M.C.C.; investigation, C.C.; resources, M.C.C.; data curation, C.C.; writing—original draft preparation, M.C.C., C.C. and L.R.; writing—review and editing, C.C. and L.R.; visualization, C.C.; supervision, L.R.; project administration, L.R. All authors have read and agreed to the published version of the manuscript.

Funding: This research received no external funding.

Data Availability Statement: The data presented in this study are available on request from the corresponding author.

Conflicts of Interest: Authors declare no conflicts of interest.

References

1. Cornell, R.M.; Schwertmann, U. *The Iron Oxides: Structure, Properties, Reactions, Occurrences, and Uses*; Wiley-Vch: Weinheim, Germany, 2003; Volume 664.
2. Dayet, L. Invasive and non-invasive analyses of ochre and iron-based pigment raw materials: A methodological perspective. *Minerals* **2021**, *11*, 210. [CrossRef]
3. Matteini, M.; Moles, A. *La Chimica Nel Restauro*; Nardini: Firenze, Italy, 1989.
4. Watts, I. Ochre and Human Evolution. In *The International Encyclopedia of Anthropology*; Wiley-Blackwell: Hoboken, NJ, USA, 2018; pp. 1–7.
5. Elias, M.; Chartier, C.; Prévot, G.; Garay, H.; Vignaud, C. The colour of ochres explained by their composition. *Mater. Sci. Eng. B* **2006**, *127*, 70–80. [CrossRef]
6. Eastaugh, N.; Walsh, V.; Chaplin, T.; Siddall, R. *Pigment Compendium: A Dictionary of Historical Pigments*; Routledge: Oxford, UK, 2007.
7. Montagner, C.; Sanches, D.; Pedroso, J.; Melo, M.J.; Vilarigues, M. Ochres and earths: Matrix and chromophores characterization of 19th and 20th century artist materials. *Spectrochim. Acta Part A Mol. Biomol. Spectrosc.* **2013**, *103*, 409–416. [CrossRef]
8. Mastrotheodoros, G.P.; Beltsios, K.G. Pigments—Iron-based red, yellow, and brown ochres. *Archaeol. Anthrop. Sci.* **2022**, *14*, 35. [CrossRef]
9. Cavallo, G.; Fontana, F.; Gialanella, S.; Gonzato, F.; Riccardi, M.P.; Zorzin, R.; Peresani, M. Heat treatment of mineral pigment during the upper Palaeolithic in north-east Italy. *Archaeometry* **2018**, *60*, 1045–1061. [CrossRef]
10. Fragoso, D.; Costa, S.; Martins, E.; Dias, F.R.; Rosas, P.; Candeias, A.; Carvalho, M.L.; Manso, M. Through the hermit—Rediscovering António Dacosta's lost painting. *Microchem. J.* **2016**, *126*, 474–479. [CrossRef]
11. Townsend, J.H. The materials of JMW Turner: Pigments. *Stud. Conserv. J.* **1993**, *38*, 231–254.
12. Kampasakali, E.; Papliaka, Z.E.; Christofilos, D.; Varella, E.A. The Russian Avant-Garde Painting Palette Documentary and Physicochemical Study of Inorganic Colorants. *J. Anal. Env. Cult. Herit. Chem.* **2007**, *97*, 447–472. [CrossRef]
13. Ferro, D. The authenticity of the false. Substantia. *Int. J. Hist. Chem.* **2019**, *3*, 17–27.
14. Gerstenblith, P. Provenances: Real, fake, and questionable. *Int. J. Cult. Prop.* **2019**, *26*, 285–304. [CrossRef]
15. Giannossa, L.C.; Laviano, R.; Mastrorocco, F.; Giannelli, G.; Muntoni, I.M.; Mangone, A. A pottery jigsaw puzzle: Distinguish true and false pieces in two Apulian red figured vases by a poli-technique action plan. *App. Phys. A* **2016**, *122*, 68. [CrossRef]
16. Aura Tortosa, J.E.; Gallello, G.; Roldan, C.; Cavallo, G.; Pastor, A.; Murcia-Mascarós, S. Characterization and sources of Paleolithic–Mesolithic ochre from Coves de Santa Maira (Valencian Region, Spain). *Geoarchaeology* **2021**, *36*, 72–91. [CrossRef]
17. Lebon, M.; Gallet, X.; Bondetti, M.; Pont, S.; Mauran, G.; Walter, P.; Bellot-Gurlet, L.; Puaud, S.; Zazzo, A.; Forestier, H.; et al. Characterization of painting pigments and ochres associated with the Hoabinhian archaeological context at the rock-shelter site of Doi Pha Kan (Thailand). *J. Archaeol. Sci. Rep.* **2019**, *26*, 101855. [CrossRef]
18. Mortimore, J.L.; Marshall, L.J.R.; Almond, M.J.; Hollins, P.; Matthews, W. Analysis of red and yellow ochre samples from Clearwell Caves and Çatalhöyük by vibrational spectroscopy and other techniques. *Spectrochim. Acta Part A Mol. Biomol. Spectrosc.* **2004**, *60*, 1179–1188. [CrossRef]
19. Capel, J.; Huertas, F.; Pozzuoli, A.; Linares, J. Red ochre decorations in Spanish Neolithic ceramics: A mineralogical and technological study. *J. Archaeol. Sci.* **2006**, *33*, 1157–1166. [CrossRef]
20. Bikiaris, D.; Daniilia, S.; Sotiropoulou, S.; Katsimbiri, O.; Pavlidou, E.; Moutsatsou, A.P.; Chryssoulakis, Y. Ochre-differentiation through micro-Raman and micro-FTIR spectroscopies: Application on wall paintings at Meteora and Mount Athos, Greece. *Spectrochim. Acta Part A Mol. Biomol. Spectrosc.* **2000**, *56*, 3–18. [CrossRef]
21. Genestar, C.; Pons, C. Earth pigments in painting: Characterisation and differentiation by means of FTIR spectroscopy and SEM-EDS microanalysis. *Anal. Bioanal. Chem.* **2005**, *382*, 269–274. [CrossRef]
22. Bugini, R.; Corti, C.; Folli, L.; Rampazzi, L. Unveiling the use of creta in Roman plasters: Analysis of clay wall paintings from Brixia (Italy). *Archaeometry* **2017**, *56*, 84–95. [CrossRef]
23. Volpi, F.; Vagnini, M.; Vivani, R.; Malagodi, M.; Fiocco, G. Non-invasive identification of red and yellow oxide and sulfide pigments in wall-paintings with portable ER-FTIR spectroscopy. *J. Cult. Herit.* **2023**, *63*, 158–168. [CrossRef]
24. Franquelo, M.L.; Duran, A.; Herrera, L.K.; De Haro, M.J.; Perez-Rodriguez, J.L. Comparison between micro-Raman and micro-FTIR spectroscopy techniques for the characterization of pigments from Southern Spain Cultural Heritage. *J. Mol. Struct.* **2009**, *924*, 404–412. [CrossRef]
25. Guglielmi, V.; Andreoli, M.; Comite, V.; Baroni, A.; Fermo, P. The combined use of SEM-EDX, Raman, ATR-FTIR and visible reflectance techniques for the characterisation of Roman wall painting pigments from Monte d'Oro area (Rome): An insight into red, yellow and pink shades. *Env. Sci. Pollut. Res. Int.* **2022**, *29*, 29419–29437. [CrossRef] [PubMed]
26. Potter, M.J. Iron Oxide Pigments. In *U.S. Geological Survey Minerals Yearbook*; U.S. Geological Survey: Reston, VA, USA, 2002.
27. Harley, R.D. Artists' Pigments c.1600-1835. In *A Study of English Documentary Spurces*, 2nd ed.; Heinemann-Butterwoorth: London, UK, 1892.
28. Rampazzi, L.; Corti, C. Are commercial pigments reliable references for the analysis of paintings? *Int. J. Conserv. Sci.* **2019**, *10*, 207–220.
29. Barnett, J.R.; Miller, S.; Pearce, E. Colour and art: A brief history of pigments. *Opt. Laser. Technol.* **2006**, *38*, 445–453. [CrossRef]

30. Guskos, N.; Papadopoulos, G.J.; Likodimos, V.; Patapis, S.; Yarmis, D.; Przepiera, A.; Przepiera, K.; Majszczyk, J.; Typek, J.; Wabia, M.; et al. Photoacoustic, EPR and electrical conductivity investigations of three synthetic mineral pigments: Hematite, goethite and magnetite. *Mater. Res. Bull.* **2002**, *37*, 1051–1061. [CrossRef]
31. Helwig, K. Mars colours: Preparation methods and chemical composition. *Stud. Conserv.* **1998**, *43* (Suppl. S2), 23. [CrossRef]
32. Čukovska, L.R.; Minčeva–Šukarova, B.; Lluveras-Tenorio, A.; Andreotti, A.; Colombini, M.P.; Nastova, I. Micro-Raman and GC/MS analysis to characterize the wall painting technique of Dicho Zograph in churches from Republic of Macedonia. *J. Raman Spectrosc.* **2012**, *43*, 1685–1693. [CrossRef]
33. Franquelo, M.L.; Perez-Rodriguez, J.L. A new approach to the determination of the synthetic or natural origin of red pigments through spectroscopic analysis. *Spectrochim. Acta Part A Mol. Biomol. Spectrosc.* **2016**, *166*, 103–111. [CrossRef]
34. Ionescu, O.H.; Mohanu, D.; Stoica, A.I.; Baiulescu, G.E. Analytical contributions to the evaluation of painting authenticity from Princely church of Curtea de Arges. *Talanta* **2004**, *63*, 815–823. [CrossRef]
35. Li, Z.; Wang, L.; Ma, Q.; Mei, J. A scientific study of the pigments in the wall paintings at Jokhang Monastery in Lhasa, Tibet, China. *Herit. Sci.* **2014**, *2*, 21. [CrossRef]
36. Rizzo, M.M.; Machado, L.D.B.; Borrely, S.I.; Sampa, M.H.O.; Rela, P.R.; Farah, J.P.S.; Schumacher, R.I. Effects of gamma rays on a restored painting from the XVIIth century. *Radiat. Phys. Chem. Oxf. Engl.* **2002**, *63*, 259–262. [CrossRef]
37. Sawczak, M.; Kamińska, A.; Rabczuk, G.; Ferretti, M.; Jendrzejewski, R.; Śliwiński, G. Complementary use of the Raman and XRF techniques for non-destructive analysis of historical paint layers. *Appl. Surf. Sci.* **2009**, *255*, 5542–5545. [CrossRef]
38. Schenatto, J.; Rizzutto, M.A. Use of non-invasive methods of analysis applied to the study of Oscar Pereira da Silva paintings. In *Lasers in the Conservation of Artworks*; CRC Press: Boca Raton, FL, USA, 2024; Volume XIII, pp. 12–21.
39. Vermeulen, M.; Miranda, A.S.O.; Tamburini, D.; Delgado, S.E.R.; Walton, M. A multi-analytical study of the palette of impressionist and post-impressionist Puerto Rican artists. *Herit. Sci.* **2022**, *10*, 44. [CrossRef]
40. Żmuda-Trzebiatowska, I.; Wachowiak, M.; Klisińska-Kopacz, A.; Trykowski, G.; Śliwiński, G. Raman spectroscopic signatures of the yellow and ochre paints from artist palette of J. Matejko (1838–1893). *Spectrochim. Acta Part A Mol. Biomol. Spectrosc.* **2015**, *136*, 793–801. [CrossRef]
41. Marengo, E.; Liparota, M.C.; Robotti, E.; Bobba, M. Monitoring of paintings under exposure to UV light by ATR-FT-IR spectroscopy and multivariate control charts. *Vib. Spectrosc.* **2006**, *40*, 225–234. [CrossRef]
42. Buti, D.; Rosi, F.; Brunetti, B.G.; Miliani, C. In-situ identification of copper-based green pigments on paintings and manuscripts by reflection FTIR. *Anal. Bioanal. Chem.* **2013**, *405*, 2699–2711. [CrossRef] [PubMed]
43. Carlesi, S.; Becucci, M.; Ricci, M. Vibrational spectroscopies and chemometry for nondestructive identification and differentiation of painting binders. *J.Chem.* **2017**, *1*, 3475659. [CrossRef]
44. Pallipurath, A.; Skelton, J.; Ricciardi, P.; Bucklow, S.; Elliott, S. Multivariate analysis of combined Raman and fibre-optic reflectance spectra for the identification of binder materials in simulated medieval paints. *J. Raman Spectrosc.* **2013**, *44*, 866–874. [CrossRef]
45. Mazzeo, R.; Prati, S.; Quaranta, M.; Joseph, E.; Kendix, E.; Galeotti, M. Attenuated total reflection micro FTIR characterisation of pigment–binder interaction in reconstructed paint films. *Anal. Bioanal. Chem.* **2008**, *392*, 65–76. [CrossRef]
46. Miliani, C.; Rosi, F.; Daveri, A.; Brunetti, B.G. Reflection Infrared Spectroscopy for the Non-Invasive in Situ Study of Artists Pigments. *Appl. Phys. A Mater. Sci. Process.* **2012**, *106*, 295–307. [CrossRef]
47. Rampazzi, L.; Brunello, V.; Campione, F.P.; Corti, C.; Lissoni, E. Non invasive techniques for disclosing the palette of Romantic painter Francesco Hayez. *Spectrochim. Acta A* **2017**, *176*, 142–154. [CrossRef]
48. Rampazzi, L.; Brunello, V.; Campione, F.P.; Corti, C.; Geminiani, L.; Recchia, S.; Luraschi, M. Non-invasive identification of pigments in Japanese coloured photographs. *Microchem. J.* **2020**, *157*, 105017. [CrossRef]
49. Bruni, S.; Guglielmi, V.; Della Foglia, E.; Castoldi, M.; Gianni, G.B. A non-destructive spectroscopic study of the decoration of archaeological pottery: From matt-painted bichrome ceramic sherds (southern Italy, VIII-VII BC) to an intact Etruscan cinerary urn. *Spectrochim. Acta Part A Mol. Biomol. Spectrosc.* **2018**, *191*, 88–97. [CrossRef]
50. Guglielmi, V.; Fermo, P.; Andreoli, M.; Comite, V. A multi-analytical survey for the identification of the red and yellow pigments of coloured sherds discovered in the Monte d'Oro area (Rome). In *2020 IMEKO TC-4 International Conference on Metrology for Archaeology and Cultural Heritage*; International Measurement Confederation: Budapest, Hungary, 2020; pp. 548–553.
51. Monnier, G.F. A review of infrared spectroscopy in microarchaeology: Methods, applications, and recent trends. *J. Archaeol. Sci. Rep.* **2018**, *18*, 806–823. [CrossRef]
52. Liu, G.L.; Kazarian, S.G. Recent advances and applications to cultural heritage using ATR-FTIR spectroscopy and ATR-FTIR spectroscopic imaging. *Analyst* **2022**, *147*, 1777–1797. [CrossRef] [PubMed]
53. Rosi, F.; Cartechini, L.; Sali, D.; Miliani, C. Recent trends in the application of Fourier Transform Infrared (FT-IR) spectroscopy in Heritage Science: From micro-to non-invasive FT-IR. *Phys. Sci. Rev.* **2019**, *4*, 20180006. [CrossRef]
54. Kremer Pigmente. Available online: https://www.kremer-pigmente.com/it/ (accessed on 2 August 2024).
55. Fabriano. Available online: https://fabriano.com (accessed on 2 August 2024).
56. Zecchi, Soluzioni per Artisti, Materiale per Restauro. Available online: https://zecchi.it (accessed on 2 August 2024).
57. Hakeem, N.A.; Basily, A.B.; Sagr, N.; Moharram, M.A. Study of the thermal transformation of natural goethite using infrared spectroscopy. *J. Mater. Sci.* **1986**, *5*, 4–6. [CrossRef]
58. Rampazzi, L.; Corti, C.; Geminiani, L.; Recchia, S. Unexpected findings in 16th century wall paintings: Identification of aragonite and unusual pigments. *Heritage* **2021**, *4*, 2431–2448. [CrossRef]

59. Rochester, C.H.; Topham, S.A. Infrared study of surface hydroxyl groups on goethite. *J. Chem. Soc. Faraday Trans.* **1979**, *75*, 591–602. [CrossRef]
60. Ghosh, M.K.; Poinern, G.E.J.; Issa, T.B.; Singh, P. Arsenic adsorption on goethite nanoparticles produced through hydrazine sulfate assisted synthesis method. *Korean J. Chem. Eng.* **2012**, *29*, 95–102. [CrossRef]
61. Longa-Avello, L.; Pereyra-Zerpa, C.; Casal-Ramos, J.A.; Delvasto, P. Study of the calcination process of two limonitic iron ores between 250 °C and 950 °C. *Rev. Fac. Ing.* **2017**, *26*, 33–45. [CrossRef]
62. Wilson, M.J. *Clay Mineralogy: Spectroscopic and Chemical Determinative Methods*; Chapman & Hall: London, UK, 1994.
63. Cui, H.; Ren, W.; Lin, P.; Liu, Y. Structure control synthesis of iron oxide polymorph nanoparticles through an epoxide precipitation route. *J. Exp. Nanosci.* **2013**, *8*, 869–875. [CrossRef]
64. Das, S.; Hendry, M.J.; Essilfie-Dughan, J. Adsorption of selenate onto ferrihydrite, goethite, and lepidocrocite under neutral pH conditions. *J. Appl. Geochem.* **2013**, *28*, 185–193. [CrossRef]
65. Davantès, A.; Costa, D.; Lefèvre, G. Molybdenum (VI) adsorption onto lepidocrocite (γ-FeOOH): In situ vibrational spectroscopy and DFT+ U theoretical study. *J. Phys. Chem. C.* **2016**, *120*, 11871–11881. [CrossRef]
66. Frost, R.L.; Mako, E.; Kristof, J.; Kloprogge, J.T. Modification of kaolinite surfaces through mechanochemical treatment—A mid-IR and near-IR spectroscopic study. *Spectrochim. Acta Part A Mol. Biomol. Spectrosc.* **2002**, *58*, 2849–2859. [CrossRef]
67. Zhang, J.; Cheng, H.; Liu, Q.; He, J.; Frost, R.L. Mid-infrared and near-infrared spectroscopic study of kaolinite-potassium acetate intercalation complex. *J. Molec. Struct.* **2011**, *994*, 55–60. [CrossRef]
68. Bishop, J.; Madejova, J.; Komadel, P.; Fröschl, H. The influence of structural Fe, Al and Mg on the infrared OH bands in spectra of dioctahedral smectites. *Clay. Miner.* **2002**, *37*, 607–616. [CrossRef]
69. Busca, G.; Lorenzelli, V.; Ramis, G.; Willey, R.J. Surface sites on spinel-type and corundum-type metal oxide powders. *Langmuir* **1993**, *9*, 1492–1499. [CrossRef]
70. Kiskira, K.; Papirio, S.; Mascolo, M.C.; Fourdrin, C.; Pechaud, Y.; van Hullebusch, E.D.; Esposito, G. Mineral characterization of the biogenic Fe (III)(hydr) oxides produced during Fe (II)-driven denitrification with Cu, Ni and Zn. *Sci. Total Environ.* **2019**, *687*, 401–412. [CrossRef]
71. Krehula, S.; Štefanić, G.; Zadro, K.; Krehula, L.K.; Marciuš, M.; Musić, S. Synthesis and properties of iridium-doped hematite (α-Fe2O3). *J. Alloys Compd.* **2012**, *545*, 200–209. [CrossRef]
72. Vargas, M.A.; Diosa, J.E.; Mosquera, E. Data on study of hematite nanoparticles obtained from Iron (III) oxide by the Pechini method. *Data Brief* **2019**, *25*, 104183. [CrossRef]
73. Yariv, S.; Mendelovici, E. The effect of degree of crystallinity on the infrared spectrum of hematite. *App. Spectrosc.* **1979**, *33*, 410–411. [CrossRef]
74. Alp, Z.; Ciccola, A.; Serafini, I.; Nucara, A.; Postorino, P.; Gentili, A.; Curini, R.; Favero, G. Photons for Photography: A First Diagnostic Approach to Polaroid Emulsion Transfer on Paper in Paolo Gioli's Artworks. *Molecules* **2022**, *27*, 7023. [CrossRef] [PubMed]